Heat and Mass Transfer in Fixed and Fluidized Beds of Large Particles

R. D. BRADSHAW and J. E. MYERS

Purdue University, West Lafayette, Indiana

Fluid-solids contacting has been of importance in many operations since the beginning of the chemical industry. Before 1940, however, applications and research in this field were restricted to systems in which the solids formed a fixed bed. Since then much attention has been paid to the behavior of fluidized beds because of the importance of fluidized catalytic crackers. These units operate with very small catalyst particles so that fluidization research has been restricted almost entirely to studies with particles somewhat less than 0.1 in. in diam. In recent years, however, other industries have used fluidization techniques for operations such as calcination of limestone, ore recovery and roasting, drying and sizing of coal and limestone, and drying of salt. These operations necessarily involve much larger particles than those used in previously reported investigations, and there is little published information available on pressure drop and heat and mass transfer characteristics of these systems. The present work was undertaken to remedy this deficiency.

Because the technology of fixed-bed operations is well established, it was decided to begin the work with fixed-bed studies. When the experimental techniques were developed to the point at which results for fixed beds checked the published results in the literature, the work was then extended to the fluidized region. Velocities as high as four times the minimum fluidizing velocity were obtained with spheres and cylinders ranging in diameter from 0.160 to 0.335 in. and varying in specific gravity from 0.91 to 1.98. The particles were porous catalyst carriers obtained from commercial suppliers. They were soaked with water so that temperature and humidity measurements could be used to determine heat and mass transfer coefficients. Thus the information obtained has direct application in the field of fluidized drying as well as providing basic information on the heat and mass transfer behavior of fluidized systems of large particles.

As indicated earlier, a large amount of information is available in the literature on pressure drop and heat and mass transfer characteristics of fixed and fluidized beds. The volume of this literature is so great that a summary of it is given elsewhere (3). The only references cited here will be those which are either very recent or especially pertinent. These are referred to in the discussion of results where comparisons with results of the present investigation are given.

R. D. Bradshaw is with General Dynamics/Astronautics, San Diego, California.

EXPERIMENTAL APPARATUS

A schematic diagram of the apparatus is given in Figure 1. The two columns used were of standard 6- and 12-in. pipe, flanged at each end. Each had a flow-smoothing section of 2 in. of small steel spheres in a section preceding the bed entrance. The beds were supported on an aluminum plate perforated with 1/16-in. holes. A sector was removed from the length of each pipe and replaced with a concave Lucite sector so that the fluidized-bed behavior might be observed. A handhole for charging the bed was likewise covered with concave Lucite. The columns and all piping were insulated with fiberglas insulation.

The air source was a blower capable of providing 300 std. cu. ft./min. at 15 lb./sq. in. gauge. The air temperature was controlled by a finned cooler. The flow was metered with a rotameter of 325 cu. ft./min. capacity. The columns, air metering section, and humidity-determination sections were connected with 1½-in. piping.

The humidities at inlet and outlet to the bed were determined with dry and wet-bulb thermocouples. The wet-bulb thermocouple was a single strand wire, shaped in the form of the letter *D* and butt welded at the midpoint of the straight section (*17*). The straight portion was covered with a twill wick which led into the reservoir. The humidity measurements were checked on several occasions with drying agents, and an error less than 1% was present on the average. A mixing baffle arrangement followed by an aluminum elbow 1½ in. in diam. provided a continuous sampling of outlet air from the bed. The air flow over the wicks was maintained at 15 ft./sec. by passing inlet and outlet samples through rotameters after the humidity was determined. Iron-constantan thermocouples were used, and temperatures were measured with both a recorder and a potentiometer. The temperature at the bed entrance was also measured since temperature sometimes varied between the inlet sample point and the bed entrance.

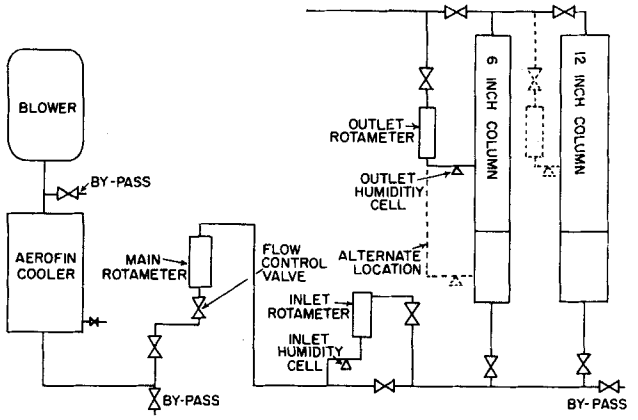

Fig. 1. Schematic diagram of apparatus.

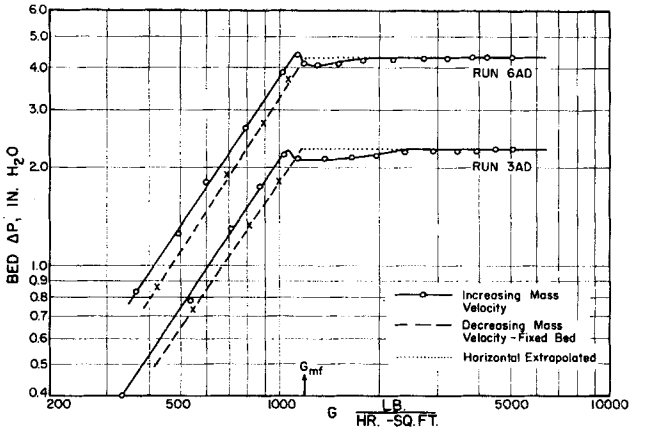

Fig. 2. Fluidized bed pressure drop vs. mass velocity.

A network of pressure taps and lines was used to measure static pressure at rotameters, humidity cells, and at the columns. Pressure drops for various bed increments were also determined. The water manometer used to measure the bed pressure drop had a valve in the bottom U-section of the manometer to reduce fluctuations to facilitate reading.

After testing some fifteen types of particles, three types were selected. The particles used in this work were Celite 410 and Celite 408 cylinders, Kaosorb cylinders, Kao-Spheres, and AMT spheres. These were selected because of good attrition resistance and high porosity. The Celite particles have the added advantage of color change on drying. The important properties of the particles, which find a wide industrial use as catalyst carriers, are presented in Table 1.

EXPERIMENTAL PROCEDURE

The friction data were taken with dry pellets since density varied during a run as the soaked pellets dried. Heat and mass transfer runs were made later with soaked pellets; the two types of runs will be discussed separately. The baffles and outlet-humidity measuring apparatus were not present for friction runs. The mixing baffles tended to interfere with deep beds and the outlet screen became fouled.

For each pressure drop run with a charge of dry pellets, the mass velocity was increased or decreased by increments to give conditions of fixed bed, minimum fluidization, fluidized bed, and fluidization up to a maximum air flow. At each flow setting, pressure drop and maximum and minimum bed heights were recorded as well as other pressure and temperature data necessary to determine the flow rate. Fixed-bed heights for Celite 410 ranged from 2 to 9 in. and fluidized heights were as high as 21 in. For the remainder of the particles, initial bed heights of 3 and 6 in. were used. Downflow as well as upflow runs were made in the 6-in. column to obtain high mass velocities in the fixed beds. In the 12-in. column, the air supply limited the investigation to static-bed studies.

Before the series of heat and mass transfer runs commenced, several preliminary tests were undertaken. It was necessary to know the length of the constant-rate drying period for the pellets and, knowing this, to determine when to record the data. After many tests at different flow rates and pellet charges, it was decided to use data recorded after 60% of the constant-rate period was over. The constant-rate periods ranged from 3 to 30 min. in duration. Tests indicated that prior to the 60% point of the run, moisture was blown from the bed in droplet form; this gave an interfacial area greater than that of the porous particles in the bed.

A second test was made to determine if the particle surface temperature was actually the wet-bulb temperature. Thermocouples were placed both in bored out pellets and in proximity to pellet surfaces within a cluster of pellets; the latter was for use when air flow was suddenly shut off. Representative values obtained indicated an error of 0.4°F. at 2.8 ft./sec. superficial velocity and no determinable error at 8 ft./sec. This is confirmed by work of DeAcetis and Thodos at low velocities (5). For the present work, 95% of the data were taken at velocities greater than 4 ft./sec. Thus, pellet surfaces were taken to be at wet-bulb temperature.

A heat and mass transfer run consisted of drying one bed of pellets. Pellets were soaked for 24 hr. Then the water was poured off and surface droplets were removed with a cloth prior to placing them in the bed. A total of 220 runs were made in random order. Bed heights ranged from 1 to 6 in., but only at high flow rates were the deeper beds used. It had been reported eariler that greater than 90% approach to saturation gave unreliable results (4). The inlet air was maintained near room temperature; but at the start of a run both the pellets and the column were near wet-bulb temperature. The column was cooled by operating with a bag of moist pellets just prior to the run.

Detailed procedure for a run involved allowing the air to reach a steady temperature at the selected flow rate. After the column was cooled, the humidity cell wicks were sprayed to remove dust and the pellets were placed in the column. Temperatures were measured during the run at intervals of a minute, pressure drop and static pressures were recorded, and maximum and minimum bed heights were noted. Initial and final bed weights gave a satisfactory check of drying rate. Most beds were fluidized prior to a static run to give a reproducible reading of void fraction in the static beds.

TABLE 1. PARTICLE PROPERTIES

Property	Celite 410 cylinders	Celite 408 cylinders	Kaosorb cylinders	Kao-Spheres	AMT spheres
Dimensions, in.	0.243 × 0.192	0.166 × 0.167	0.159 × 0.163	0.177 × 0.207	0.345
D_p, in.	0.223	0.166	0.160	0.185	0.345
ρ_s, lb. dry/cu. ft.	59.29	56.63	80.90	77.26	123.7
A_s, sq. ft./lb.dry	5.44	7.64	5.55	5.05	1.69
Moisture after soaking, lb./lb. dry	0.624	0.662	0.384	0.416	0.190
Equil. moisture cont., lb./lb. dry	0.0020	0.0035	0.0230	0.0234	0.0005
Attrition after 1 hr., mass percent	0.88	0.88	0.15	0.15	2.10

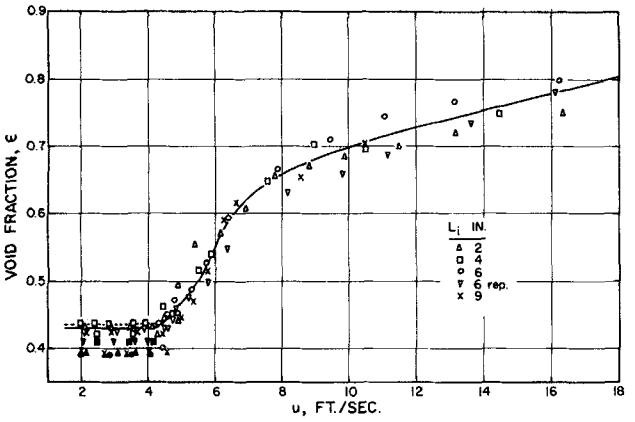

Fig. 3. Void fraction variation with velocity for Celite 410 friction runs.

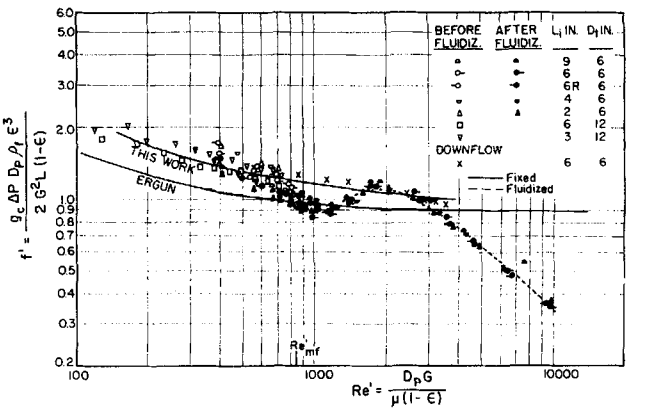

Fig. 4. Friction factor f' vs. modified Reynolds number for Celite 410 cylinders.

FRICTION FACTOR RESULTS

Typical behavior for plots of ΔP vs. G was observed in this work; an example using 3- and 6-in. beds of Kao-Spheres is shown in Figure 2. The results indicated that G_{mf} was not a function of bed height. In plots such as Figure 2, no trend away from horizontal as reported by Miller (*15*) was detected when mass velocity was increased to values as great as 4 G_{mf}.

The definition of the friction factor, f', used for this work is

$$f' = \frac{g_c \, \Delta P \, D_p \, \rho_f \, \epsilon^3}{2 \, G^2 \, L \, (1 - \epsilon)} \qquad (1)$$

The large effect of void fraction on f' in this definition is obvious. It was observed from a study of the void fraction values for fluidized beds that the values of ϵ varied randomly independent of initial bed height as shown in Figure 3; thus it was concluded that void fraction was not a discernible function of bed height. Therefore, to minimize the effect of scatter in void fraction results, all void fraction data for each particle size were smoothed with a curve such as Figure 3 for Celite 410 particles. Neither a straight line on an arithmetic or on a log-log plot (*13, 14, 18*) fitted the data satisfactorily, so a curve was drawn through the data to remove random variation in void fraction. At a value of $\epsilon = 1.0$, the curves were defined by Newton's law (*12*); the terminal velocity for Celite 410 was 37.6 ft./sec.

The friction factor data for the fixed beds in this work were satisfactorily represented by Ergun's equation (*7*)

$$f' = \frac{75}{N_{Re'}} + 0.875 \qquad (2)$$

where $N_{Re'}$ is a modified Reynolds number equal to $N_{Re}/(1 - \epsilon)$. The results for both fixed and fluidized beds are given as f' vs. $N_{Re'}$ on the same plot. Results for Celite 410 are presented in Figure 4 and are typical of the results for all the other particle sizes (*3*). Morse (*16*) first observed a hump in this type of curve where transition to a fluidized bed occurs. The data for five types of particle are distributed about Ergun's correlation for all except the highest Reynolds numbers. Although a comparison is not shown on Figure 4, the static-bed results from this work are in good agreement with work for spheres by Gamson et al. (*8*), and Baumeister and Bennett (*1*).

This study of friction data was made to obtain some knowledge of the behavior of large particles in fluidized systems. As has long been known, friction data scatter more widely than heat or mass transfer data because of the sensitivity to packing configuration. Correlations relating momentum transfer to heat and mass transfer for static and fluidized beds have been unsuccessful because of the complex nature of the beds and the undeterminable ratio of skin friction to form drag.

HEAT AND MASS TRANSFER COEFFICIENTS

These coefficients are discussed together since the heat transfer coefficients were not independent of the mass transfer coefficients. The coefficients determined in this work are defined by

$$q = h \, A \, (t_s - t_g)_m \qquad (3)$$

$$W(H_i - H_o) = k' \, A (H_s - H_g)_m \qquad (4)$$

The humidities were evaluated from psychrometric tables (*22*) corrected to total pressure in the bed. The mean driving force was taken as the log-mean of the driving forces at the bed inlet and outlet.

The values of k' calculated in this manner indicated an effect of bed height, with values of the coefficient as much as 40% lower occurring for deeper beds. When the possibility of axial mixing was considered for the fixed-bed data it was found that the Epstein correction factor (*6*) increased all values approximately 5 to 10%. Since the correction was smaller for deep beds, this correction only aggravated the situation of coefficients decreasing with bed height. Further, the model of perfect mixing cell is questionable for fluidized beds; hence the Epstein correction factors were not used for either fixed or fluidized beds.

The possibility of an error in the driving force was considered next. With results from different bed heights, the profiles of outlet temperature were reconstructed for both upflow fluidized beds and downflow fixed beds. When a log-mean driving force was determined for a deep bed, such as a 5-in bed, from inlet and outlet temperatures, a profile was fixed for the entire bed. Such a log-mean curve was compared with a curve through measured outlet temperatures of beds of different heights. It became apparent that the log-mean curve gave values for outlet temperature that were too high for intermediate-height beds. A better method of handling the data follows. The area under the curve is a measure of the integrated driving force, therefore a ratio of the area under the log-mean curve for each bed height to the area under the curve with results measured with incremental bed depths gave a correction factor for the coefficients for that run. Coefficients obtained by this method indicated no effect of bed height, and the average value of the coefficients obtained for several bed

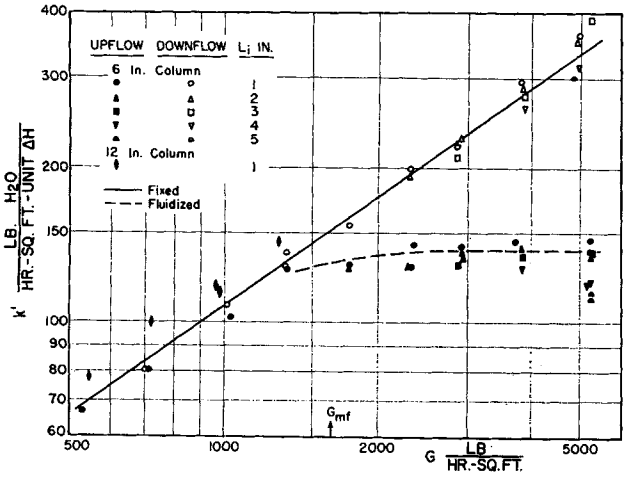

Fig. 5. Mass transfer coefficient k' vs. mass velocity for Celite 410 cylinders.

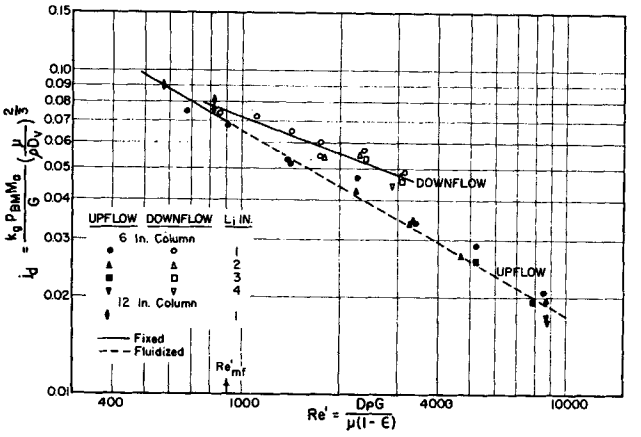

Fig. 6. Mass transfer factor j_d vs. modified Reynolds number for Kao-Spheres.

heights gave outlet temperatures near the incremental values for all bed heights. These values indicated that for deep beds, where outlet temperature was near saturation, outlet temperature readings, perhaps affected by wall heat transfer effects, may have been slightly high. Since most of the data were taken in shallow beds, this experimental error would not seriously affect the heat and mass transfer coefficients. Results in the next section are values corrected in this manner. The correction ratio for each run was applied to values for h, j_h, k', k_g, and j_d since these are related variables.

The variation of the mass transfer coefficient, k', with mass velocity is seen in Figure 5. The static-bed results fall on a straight line indicating a dependence on $G^{0.71}$, and the fluidized bed values are essentially independent of mass velocity. This was found to be true for all the particles studied and is analogous to the independence of pressure drop indicated in Figure 2. Because of the relationship for this system, $h/k' = 0.243$, the values of the heat transfer coefficient would exhibit a similar behavior.

Not all authors agree on the independence of h and k' with mass velocity in fluidized beds. Wamsley and Johanson (*21*) are the only workers to report this independence for heat transfer coefficients which Leva (*12*) calls "the unlikely result." For fluidized beds of nearly equal particle size, $D_p = 0.014$ to 0.043 in., disagreement on the dependence of mass velocity and particle diameter is exhibited by the following authors: Heertjes and McKibbens (*10*) report h proportional to $G^{0.76}\ D_p^{0.67}$; Kettenring, Manderfield, and Smith (*11*) recommend $G^{1.30}\ D_p^{0.3}$; Walton, et al. (*20*) report $G^{1.7}\ D_p^{0.1}$. The disagreement between these correlations is large. The present investigation shows the heat transfer coefficients to be approximately proportional to $D_p^{0.3}$ over the twofold range of particle diameter covered in this work, and nearly independent of G. The investigation was not aimed primarily at studying the effect of varying the particle diameter so the conclusions regarding this variable are only tentative. Mass velocities ranging up to 4 G_{mf} were studied in support of the information obtained concerning this variable.

For fluidized mass transfer work, Kettenring, Manderfield, and Smith as well as Chu, Kalil, and Wetteroth (*4*) found the mass transfer coefficient to increase with increasing mass velocity. However, with liquid fluidized beds, McCune and Wilhelm (*14*) found that the mass transfer coefficients passed through a maximum and decreased as mass velocity increased; the results with Kaosorb and Celite 408 cylinders in this work slightly suggested such behavior. These apparent discrepancies between investigators have left doubt as to the actual effect of increasing mass velocity. Fluidized systems are quite complex, and variables such as D_t, D_p, L, and ρ_s may all affect the fluidizing behavior. However, in view of the results obtained with all five particle sizes, it is concluded that the heat and mass transfer coefficients for this work in the fluidized beds were independent of mass velocity.

j FACTOR CORRELATIONS

The statistical analysis of the data was performed on the variables j_d and N_{Re} or $N_{Re'}$. From the relationship

$$\frac{j_h}{j_d} = \frac{(h/C_pG)\,(N_{Pr})^{2/3}}{(k'/G)\,(N_{Sc})^{2/3}} \qquad (5)$$

the empirical mass and heat transfer equations were related. For the air-water system in the temperature range of this work, j_h/j_d was assumed constant at 1.12. The results of the analysis for Kao-Spheres are given in Figure 6. The downflow fixed beds have higher coefficients because they have not been fluidized prior to the run and have a denser packing. This hypothesis is further confirmed by the fact that the pressure drops were lower for upflow runs than for downflow fixed-bed runs when they were

TABLE 2. REGRESSION VALUES FOR j_d VS. $N_{Re'}$ IN EQUATION (6)

Particle	Upflow, both fixed and fluidized beds			Downflow, fixed beds		
	a	b	% std. dev.	a	b	% std. dev.
Celite 410 cylinders	2.29	−0.519	±8.2	0.547	−0.300	4.2
Celite 408 cylinders	2.70	−0.554	±10.1	1.163	−0.405	4.4
Kaosorb cylinders	2.48	−0.548	±9.3	1.299	−0.437	9.9
Kao-Spheres	3.49	−0.575	±7.7	0.698	−0.376	5.4
AMT spheres	1.29	−0.421	±5.8	0.725	−0.322	3.3
All sizes	1.92	−0.496	±18.6	0.470	−0.280	13.9

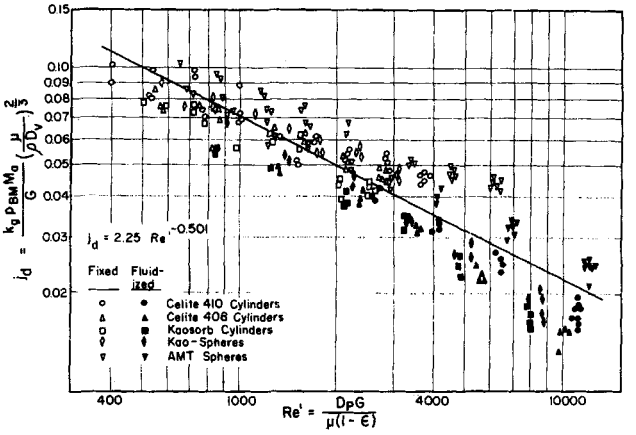

Fig. 7. Mass transfer factor j_d vs. modified Reynolds number for all runs.

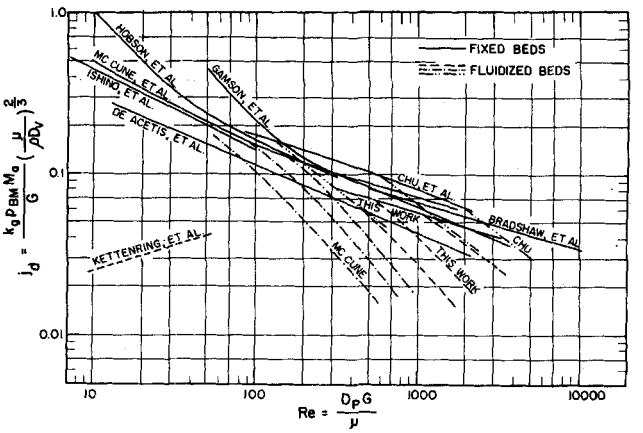

Fig. 9. Correlation of literature data—j_d vs. Re.

compared at equal mass velocities below G_{mf}. The difference between slopes for upflow and downflow is probably also caused by packing arrangement. For example, the 12-in. column runs were not fluidized and although they are upflow runs, the slope is nearly equal to the downflow slope, and the values of the coefficients fall above the upflow line in Figure 6. The 12-in. column data were not considered in the satistical analysis since they were not fluidized prior to the fixed-bed runs.

The upflow and downflow data for the 6-in. column were analyzed separately and a least-squares fit of the data made for equations of the form

$$j_d = a\ (N_{Re'})^b \qquad (6)$$

The values for a and b are given in Table 2 for upflow and downflow, respectively. The standard deviations are considered to be low for the type of experiment involved. Effects of different particles were statistically significant to the extent that the data should not be represented by a single line. However, all the data are presented together in Figure 7 and a best-fitting straight line (found by the method of least squares) is shown. The equation of the line is

$$j_d = 2.25\ (N_{Re'})^{-0.501} \qquad (7)$$

The Kao-Sphere coefficients have values about 12% greater than the Kaosorb cylinders which is indicative of higher coefficients for spherical particles. This is in agreement with the results of others who use a particle shape factor to account for the difference. Similarly, coefficients for the AMT particles were larger than for the other particles used.

The present work is compared with previous heat transfer work in Figure 8 where j_h is plotted as a function of N_{Re}. This form of Reynolds number is used since few data have been reported with $N_{Re'}$. Both Gamson, et al. (8) and DeAcetis and Thodos (5) worked with Celite particles in fixed beds and good agreement is indicated with this work. Baumeister and Bennett (1) and Glaser and Thodos (9) heated steel spheres dielectrically in packed beds. The high Reynolds number range makes comparison with other fluidized-bed work difficult. The fluidized work by other authors represented in Figure 8 was performed with much smaller particles and at lower velocities.

A comparison is available for j_d as a function of N_{Re} plotted in Figure 9. The present work agrees well with fluidized-bed studies by McCune and Wilhelm (14) with the 2-napthol-water system, and by Chu, et al. (4) with the naphthalene-air system. These authors observed an effect of particle diameter and used it as a parameter. The present fixed-bed work is also in accord with that of Bradshaw and Bennett (2) in fixed beds with the naphthalene-air system.

Fluidized-bed data are best presented on a plot where the abscissa is $N_{Re'}$. Few authors give sufficient data to obtain this correlation; however, the available data are shown in Figure 10. Again the present work is in good agreement with the correlation by Chu, et al. (4) for fixed and fluidized beds over a wide range of $N_{Re'}$. The fixed-bed correlation of Shulman, et al. (19) with the naphthalene-air system is shown, as is that of Bradshaw and Bennett with fixed beds.

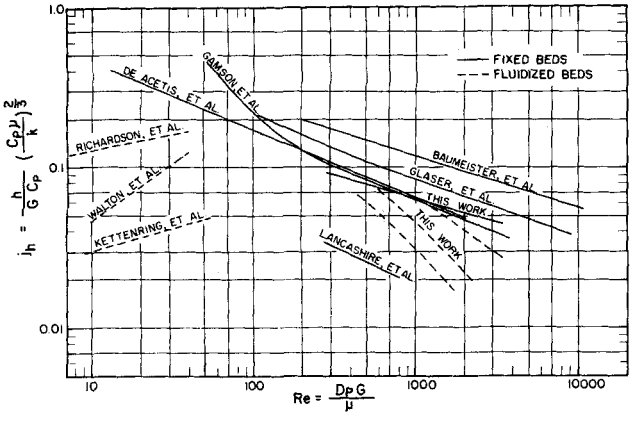

Fig. 8. Correlation of literature data—j_h vs. Re.

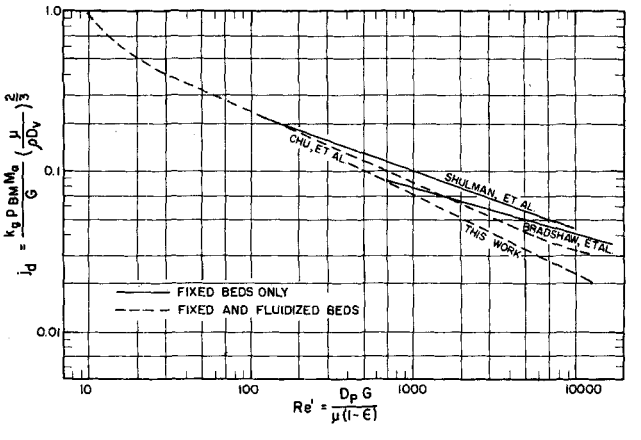

Fig. 10. Correlation of literature data—j_b vs. Re'.

SUMMARY

The evaporation of water from porous particles makes a convenient and simple system for studying mass and heat transfer in fixed and fluidized beds. However, precautions must be taken to ensure that the particle surfaces are at the wet-bulb temperature, that moisture droplets are not blown free from the porous particles, and that the particles are in the constant-rate drying period.

The log-mean driving force is satisfactory for determining heat and mass transfer coefficients when the ratio of inlet to outlet driving force is not large; that is, less than 6. For higher values of this ratio the log-mean driving force is affected significantly by small errors in measuring outlet gas temperature.. When this is avoided it appears that there is no effect of bed height on the mean values of the heat and mass transfer coefficients.

Over the range of 1 to 4 times the minimum fluidization velocity, the heat and mass transfer coefficients are independent of gas velocity. For fixed beds the coefficients are proportional to $G^{0.7}$.

The correlation of Ergun for friction factors adequately represents the fixed-bed results. However, a hump appears in the friction factor vs. modified Reynolds number curve at incipient fluidization. At flow rates above this point the friction factor is strongly dependent on modified Reynolds number.

A statistical treatment of the heat and mass transfer results gives correlations of the j factors for the different particles. However, for each particle the same correlation represents results adequately for upflow through both fixed beds and fluidized beds.

ACKNOWLEDGMENT

The authors are grateful for the financial assistance of E. I. du Pont de Nemours and Company and the Purdue Research Foundation during this work. The generosity of Minerals and Chemical Corporation of America, who donated the Kaosorb particles, and the Carborundum Company, who donated the AMT spheres, is appreciated. The efforts of Mr. Sherwood Fox, who built major units of this equipment, are acknowledged.

NOTATION

A = transfer area in a packed bed, sq. ft.
A_s = specific surface area, sq. ft./lb. dry pellets
a = arbitrary constant, dimensionless
b = arbitrary constant, dimensionless
C_p = specific heat at constant pressure, B.t.u./(lb.)(°F.)
D_p = diameter of particle, ft.
D_v = molecular diffusivity in gas, sq. ft./hr.
f' = modified friction factor, defined in Equation (1), dimensionless
G = mass velocity, lb./(hr.)(sq. ft.)
g_c = conversion factor, (ft.)(lb.$_m$)/(lb.$_f$)(sec.)^2
H = absolute humidity, lb. water/lb. air
H_s = humidity of saturated air at t_s, lb. water/lb. air
h = heat transfer coefficient, B.t.u./(hr.)(sq. ft.)(°F.)
j_d = mass transfer factor, dimensionless
j_h = heat transfer factor, dimensionless
k = thermal conductivity, B.t.u./(hr.)(ft.)(°F.)
k' = mass transfer coefficient, lb. water/(hr.)(sq. ft.)(unit ΔH)
k_g = mass transfer coefficient, lb. mole/(hr.)(sq. ft.)(atm.)
L = bed length, ft.
L_i = initial bed length, in.
M = molecular weight, lb./lb. mole
P = total pressure, in. mercury
N_{Pr} = Prandtl number, $C_p\mu/k$, dimensionless
P_{BM} = mean partial pressure of air, in. mercury
q = rate of heat flow, B.t.u./hr.
N_{Re} = Reynolds number, D_pG/μ, dimensionless
$N_{Re'}$ = modified Reynolds number, $D_pG/\mu(1-\epsilon)$, dimensionless
N_{Sc} = Schmidt number, $(\mu/\rho D_v)$, dimensionless
T = absolute temperature, °R.
t_g = gas temperature, °F.
t_s = Wet-bulb temperature of the gas, °F.
u = superficial velocity, ft./sec.
W = air mass flow rate, lb./hr.
Δ = difference
ϵ = void fraction, dimensionless
μ = viscosity, lb./(hr.)(ft.)
ρ = density, lb./cu. ft.

Subscripts

a = air
f = fluid
g = gas
i = inlet
m = mean
mf = minimum fluidization
o = outlet
s = saturation, solid
w = wall, water

LITERATURE CITED

1. Baumeister, E. B., and C. O. Bennett, *A.I.Ch.E. Journal*, **4**, 69 (1958).
2. Bradshaw, R. D., and C. O. Bennett, *ibid.*, **7**, 48 (1961).
3. Bradshaw, R. D., Ph.D. thesis, Purdue Univ., Lafayette, Ind. (1961).
4. Chu, J. C., James Kalil, and W. A. Wetteroth, *Chem. Eng. Progr.*, **49**, 141 (1953).
5. DeAcetis, James, and George Thodos, *Ind. Eng. Chem.*, 52, 1003 (1960).
6. Epstein, N., *Can. J. Chem. Eng.*, 36, 210 (1958).
7. Ergun, Sabri, *Chem. Eng. Progr.*, **48**, 89 (1952).
8. Gamson, B.W., George Thodos, and O. A. Hougen, *Trans. Am. Inst. Chem. Engrs.*, **39**, 1 (1943).
9. Glaser, M. B., and George Thodos, *A.I.Ch.E. Journal*, **4**, 63 (1958).
10. Heertjes. P. M., and S. W. McKibbins, *Chem. Eng. Sci.*, **5**, 161 (1956).
11. Kettenring, K. N., E. L. Manderfield, and J. M. Smith, *Chem. Eng. Progr.*, **46**, 139 (1950).
12. Leva, Max, "Fluidization," McGraw-Hill, New York (1959).
13. Lewis, W. K., E. R. Gilliland, and W. C. Bauer, *Ind. Eng. Chem.*, **41**, 1104 (1949).
14. McCune, L. K., and R. H. Wilhelm, *ibid.*, **41**, 1124 (1949).
15. Miller, C. O., and A. K. Logwinuk, *ibid.*, **43**, 1220 (1951).
16. Morse, R. D., *ibid.*, **41**, 1117 (1949).
17. Powell, R. W., *Proc. Phys. Soc. (London)*, **48**, 406 (1936).
18. Richardson, J. F., and W. N. Zaki, *Trans. Inst. Chem. Engrs. (London)*, **32**, 35 (1954).
19. Shulman, H. L., C. F. Ullrich, A. Z. Proulx, and J. O. Zimmerman, *A.I.Ch.E. Journal*, **1**, 253 (1955).
20. Walton, J. S., R. L. Olsen, and O. Levenspiel, *Ind. Eng. Chem.*, **44**, 1474 (1952).
21. Wamsley, W. W., and L. N. Johanson, *Chem. Eng. Progr.*, **50**, 347 (1954).
22. Zimmerman, O. T., and I. Lavine, "Psychrometric Tables and Charts," Industrial Research Service, Dover, N. H. (1945).

Manuscript received June 6, 1962; revision received March 15, 1963; paper accepted March 18, 1963. Paper presented at A.I.Ch.E. New Orleans meeting.